Polarized Drell-Yan Measurements with the Fermilab Main Injector

L.D. Isenhower, T. Hague, R. Towell, S. Watson
Abilene Christian University, Abilene, TX 79699

C. Aidala, C. Dutta, W. Lorenzon (Co-Spokesperson), R. Raymond, Z. Qu
University of Michigan, Ann Arbor, MI 48109

J. Arrington, D. Geesaman, J.K. Hafidi, R. Holt, H. Jackson, P.E. Reimer (Co-Spokesperson), J. Rubin
Argonne National Laboratory, Argonne, IL 60439

C.N. Brown, D. Christian
Fermi National Accelerator Laboratory, Batavia, IL 60510

E. Kinney
University of Colorado, Boulder, CO 80309-0390

E.J. Beise, K. Nakahara
University of Maryland, College Park, MD 20742

S. Sawada
KEK, Tsukuba, Ibaraki 305-0801, Japan

M. Liu, X. Jiang, P. McGaughey, J. Huang
Los Alamos National Laboratory, Los Alamos, NM 87545

L. El Fassi, R. Gilman, R. Ransome, A. Tadepalli
Rutgers University, Rutgers, NJ 08544

Y. Goto
RIKEN, Wako, Saitama 351-01, Japan

S. Miyasaka, K. Nakano, F. Sanftl, T.-A. Shibata
Tokyo Institute of Technology, Tokyo 152-8551, Japan

B. Dannowitz, M. Diefenthaler, B. Kerns, N.C.R. Makins, R.E. McClellan
University of Illinois, Urbana, IL 61081

Y. Miyachi
Yamagata University, Yamagata 990-8560, Japan

(Dated: May 20, 2012)

Contents

1 Physics Motivation

The proton is a unique bound state, unlike any other yet confronted by physics. We know its constituents, quarks and gluons, and we have a theory, QCD, to describe the strong force that binds these constituents together, but two key features make it a baffling system that defies intuition: the confining property of the strong force, and the relativistic nature of the system. Real understanding of the proton can only be claimed when two goals are accomplished: precise calculations of its properties from first principles, and the development of a meaningful picture that well approximates the system's dominant behavior, likely via effective degrees of freedom.

The excitement and challenge of the quest for this intuitive picture is well illustrated by the ongoing research into the spin structure of the proton, and in particular, into the contribution from quark orbital angular momentum (OAM). As experiment provides new clues about the motion of the up, down, and sea quarks, theory continues to make progress in the interpretation of the data, and to confront fundamental questions concerning the very definition of L in this context. Yet crucial pieces are still missing on the experimental side. This proposal aims to fill in such a piece: the lack of any spin-dependent data on one of the most powerful probes of hadronic substructure available, the Drell-Yan process.

1.1 The Proton Spin Puzzle and Orbital Angular Momentum

In its simplest form, the proton spin puzzle is the effort to decompose the proton's total spin into its component parts

$$\frac{1}{2} = \frac{1}{2}\Delta\Sigma + \Delta G + L_q + L_g \,. \tag{1}$$

$\Delta\Sigma$ is the net polarization of the quarks, summed over flavor, and is known to be around 25% [1]. The gluon polarization, ΔG, is currently under study at the RHIC collider; the data collected to date favor a positive but modest contribution. What remains is the most mysterious contributions of all: the orbital angular momentum of the partons.

With the spin sum above as its capstone goal, the global effort in hadronic spin structure seeks to map out the proton's substructure at the same level of scrutiny to which the atom and the nucleus have been subjected. To this end, experiments with high-energy beams map out the proton's *parton distribution functions* (PDFs): the number densities of quarks and gluons as a function of momentum, flavor, spin, and, most recently, space. Deep-inelastic scattering (DIS) has yielded the most precise information on the unpolarized and helicity-dependent PDFs $f_1^q(x)$ and $g_1^q(x)$ for quarks. Here q represents quark flavor and includes the gluon, g, while x is the familiar Bjorken scaling variable denoting the fraction of the target nucleon's momentum carried by the struck quark. (The logarithmic dependence of the PDFs on the hard scattering scale has been suppressed for brevity.) For antiquarks, these distributions are accessed most cleanly by the Drell-Yan and W-production processes in proton-nucleon scattering. As with semi-inclusive DIS (SIDIS) or deep-inelastic jet production, both of these processes are purely leptonic in one half of their hard-scattering diagrams (see Fig. 1), which facilitates clean interpretation and enables the event-level determination of the parton kinematics. The unique sensitivity of Drell-Yan and W-production to sea quarks is clearly shown: an antiquark is needed at the annihilation vertex in both cases. The Fermilab E-866 experiment used Drell-Yan scattering to make its dramatic determination of the pronounced $\bar{d}(x)/\bar{u}(x)$ excess in the sea; the PHENIX and STAR

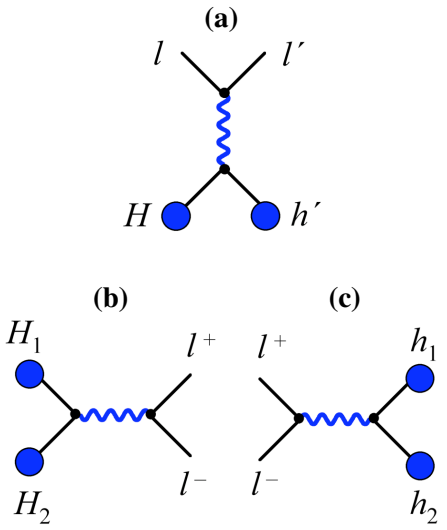

Figure 1: Tree-level hard-scattering processes of the three reactions where TMD universality has been established (a) semi-inclusive DIS (b) Drell-Yan / W-production (c) e^+e^- annihilation

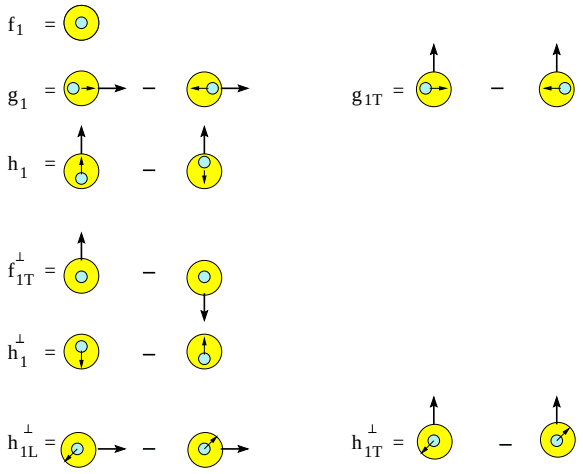

Figure 2: Operator structures of the the eight leading-twist TMDs. The horizontal direction is that of the virtual boson probing the distribution. The large and small circles represent the proton and quark respectively, while the attached arrows indicate their spin directions.

experiments at RHIC are currently measuring W-production with polarized proton beams to determine the antiquark helicity PDFs $\Delta\bar{u}(x)$ and $\Delta\bar{d}(x)$ with new precision.

Over the past decade, attention has shifted to two new classes of parton distribution functions that offer a richer description of the proton's interior than $q(x)$ and $\Delta q(x)$. These are the TMDs (Transverse Momentum Dependent PDFs) and the GPDs (Generalized Parton Distributions). The descriptions are complementary: they correlate the partons' spin, flavor, and longitudinal momentum x with transverse momentum $\mathbf{k}_T$ in the TMD case and with transverse position $\mathbf{b}_T$ in the GPD case. Both offer access to L, via different experimental approaches. The GPD approach relies on the measurement of exclusive photon and meson production with lepton beams at large Q^2. This proposal focuses on the TMDs, which are accessed most cleanly via the azimuthal distributions of the final-state products of the SIDIS and Drell-Yan processes with polarized beams and/or targets. The details of these "single-spin azimuthal asymmetries" are presented in Section 1.2.

When parton transverse momentum $\mathbf{k}_T$ is included – i.e., momentum transverse to that of the s- or t-channel virtual boson – one obtains the *transverse momentum distributions*. Theoretical analysis of the SIDIS process has led to the identification of eight such TMDs at leading twist [2, 3]. Their operator structure is shown schematically in Fig. 2. Three of these survive on integration over $\mathbf{k}_T$: the transverse extensions $f_1^q(x,\mathbf{k}_T^2)$ and $g_1^q(x,\mathbf{k}_T^2)$ of the familiar PDFs and a third distribution, $h_1^q(x,\mathbf{k}_T^2)$ termed transversity. The remaining five TMDs bring $\mathbf{k}_T$ into the picture at an intrinsic level, and vigorous theoretical work has been devoted to deciphering their significance. The most intensely studied are the Sivers [4] distribution $f_{1T}^{\perp,q}(x,\mathbf{k}_T^2)$ and the Boer-Mulders [5] distribution $h_1^{\perp,q}(x,\mathbf{k}_T^2)$. As shown in Fig. 2, they describe the correlation of the quark's momentum with the transverse spin of either the proton (Sivers) or the quark itself (Boer-Mulders). At first

sight, the operator differences depicted in the figure seem absurd: in the Sivers case, for example, how can the quark's momentum distribution change if one simply rotates the proton's spin direction by 180 degrees? A solution is presented when one considers the *orbital angular momentum* of the quarks, L_q. If the up quarks' OAM is aligned with the proton spin, then the quarks will be oncoming – blue-shifted – on *different sides* of the proton depending on its spin orientation. The search for a rigorous, model-independent connection between the Sivers distribution and quark OAM is ongoing (see Refs. [6, 7, 8] for examples of recent approaches). The connection is as yet model-dependent, but what is clear is that the existence of the Sivers function *requires* non-zero quark OAM.

1.2 Spin, L, and QCD

Orbital angular momentum provides one of the most dramatic illustrations of the challenge of understanding the most fundamental bound state of QCD, the proton. In atomic and nuclear physics, L is a conserved quantity: a good quantum number that leads to the shell structure of these familiar systems. Not so with the proton. As the masses of the light quarks are so much smaller than the energy-scale of the system (e.g. the mass of the proton itself: 938 MeV compared with the 3 MeV–5 MeV of the up and down quarks), the system is innately relativistic. In relativistic quantum mechanics, L is *not* a conserved quantity: neither it nor spin commute with even the free Dirac Hamiltonian, and so a shell structure within the proton is excluded. A simple calculation of the ground state of a light Dirac fermion bound in a central potential, for example, shows that the ground-state spinor is in a mixed state of L: $L = 0$ for the upper components and $L = 1$ for the lower components [9].

Further, the *definition* of quark OAM is under active dispute. The simple spin sum of Eq. 1 conceals a wealth of complexity in the definition of its components. Two versions of this decomposition have dominated the discussion to date. They are colloquially referred to as the Jaffe [10] and Ji [11] decompositions, though they have been addressed by numerous authors (see Refs. [12, 13] for elegant summaries of the issues).

The Ji decomposition can be expressed as

$$\vec{J}_{\text{proton}} = \int \psi^\dagger \frac{1}{2}\vec{\Sigma}\psi\, d^3x + \int \psi^\dagger \vec{x} \times \frac{1}{i}\vec{D}\psi\, d^3x + \int \vec{x} \times (\vec{E}^a \times \vec{B}^a)\, d^3x, \tag{2}$$

where a is a color index. It has three gauge-invariant terms which, in order, represent the quark spin $\Delta\Sigma$, quark OAM L_q, and total angular momentum J_g of the gluons. The advantage of this decomposition is its rigorous connection to experiment via the Ji Sum Rule [11], which relates J_q for each quark flavor q to the second moment of two GPDs

$$\vec{J}_q = \lim_{t\to 0} \int x[H_q(x,\xi,t) + E_q(x,\xi,t)]dx\,. \tag{3}$$

The actual measurement of these GPDs is an enormous experimental task; it was initiated at HERMES and will be continued with greater precision at Jefferson Laboratory and COMPASS. The Ji decomposition can also be addressed by lattice QCD, which has already been used to "measure" moments of the GPDs under certain approximations (e.g. Ref. [14]). One disadvantage of this decomposition is the lack of a gauge-invariant separation of the gluon J_g into spin and orbital pieces. A second disadvantage is the problem of *interpreting* its definition of L_q as $\vec{x} \times \vec{D}$. The appearance of the covariant derivative $\vec{D} = \vec{\nabla} + i\vec{g}$ brings

gluons into the definition. This is not the familiar, field-free OAM, $\vec{x}\times\vec{p}$, that is addressed by quark models of the proton.

The Jaffe decomposition is

$$\vec{J}_{\text{proton}} = \int \psi^\dagger \frac{1}{2}\vec{\Sigma}\psi\, d^3x + \int \psi^\dagger \vec{x}\times\frac{1}{i}\vec{\nabla}\psi\, d^3x + \int \vec{E}^a\times\vec{A}^a\, d^3x + \int E^{ai}\vec{x}\times\vec{\nabla}A^{ai}\, d^3x. \tag{4}$$

It has four gauge-invariant terms, which in order represent the quark spin, quark OAM, gluon spin, and gluon OAM. Here, L_q *is* the field-free, canonical operator $\vec{x}\times\vec{\nabla}$. The gluon spin and OAM are separated in a gauge-invariant way, and in the infinite-momentum frame, parton distribution functions for the four pieces can be defined. The disadvantage of the Jaffe decomposition is that it is unclear how to *measure* its L_q and L_g terms, either in the lab or on the lattice, as they are non-local operators unless one selects a specific gauge (the lightcone gauge, $A^+ = 0$).

At present, we are thus confronted with one definition of L_q that can be measured but not interpreted, and another that can be interpreted but not measured. The "dynamical" OAM, $\vec{x}\times\vec{D}$, of the Ji decomposition brings us face-to-face with the unique, *confining* nature of QCD: we cannot avoid interactions in a theory where quarks cannot be freed. Can we learn to interpret this quantity? This remains an open question, as only the "canonical" OAM definition, $\vec{x}\times\vec{\nabla}$, obeys the commutation relations of angular momentum algebra.

1.3 OAM in the Sea

As theory continues to wrestle with these fundamental questions, experiment continues to measure. An enticingly coherent picture of quark OAM has emerged from the measurements of the Sivers function made via polarized SIDIS by the HERMES and COMPASS collaborations [15, 16]. When subjected to a global fit [17, 8] and combined with the chromodynamic lensing model of Ref. [7], they indicate $L_u > 0$ and $L_d < 0$ [18].

This agrees with the most basic prediction of the meson-cloud model of the proton. In this model, the proton is described as a superposition of a zeroth-order bare proton state of three constituent *uud* quarks and a first-order cloud of nucleon-pion states. The seminal idea behind this model is that hadrons, not quarks and gluons, are the best degrees of freedom with which to approximate the essential features of the proton. The pion cloud has two components: $n\pi^+$ and $p\pi^0$, weighted by the Clebsch-Gordan coefficients of these two isospin combinations. Immediately, we have an explanation for the dramatic excess of $\bar{d}$ over $\bar{u}$ observed by FNAL-E-866 [19]: with the sea quarks wrapped up in the lightest hadronic states, the π^0 cloud contributes $\bar{d}$ and $\bar{u}$ in equal measure but the π^+ contributes only $\bar{d}$. Further, as the pions have zero spin, the antiquarks should be unpolarized. This agrees with the HERMES SIDIS data on $\Delta\bar{u}(x)$ and $\Delta\bar{d}(x)$ [20], both of which were found to be consistent with zero.

The meson cloud's picture of orbital angular momentum is dramatic. As the constituents are heavy in this picture, non-relativistic quantum mechanics applies and L is once again a good quantum number. In what state of L is the pion cloud? The pions have negative parity while the nucleons have positive parity. To form a positive-parity proton from $n\pi^+$ or $p\pi^0$, the pions must carry $L = 1$. The lowest-order prediction of the meson cloud model is thus of an *orbiting cloud*; application of Clebsch-Gordan coefficients yields $L_u > 0$

and $L_d < 0$ [18, 21].

Unfortunately, this apparently coherent picture is at odds with lattice calculations, which give $L_u < 0$ and $L_d > 0$ at the Q^2 scales of the Sivers measurements [22]. Recent work from a number of directions suggests that the resolution of this puzzle lies in the proton *sea*. As the sea quarks' spin polarization is near zero, and as the sea quarks' disconnected diagrams are difficult to treat on the lattice, a tendency to neglect them has emerged in the spin community. As a result, the simple fact has eluded us that the L_u and L_d determined from quark models and from SIDIS data refer to quarks only, while the lattice calculations include *both* quarks and antiquarks of the given flavor. Several recent developments have highlighted the perils of this bias. First, data from HERMES and BRAHMS on single-spin azimuthal asymmetries for kaon production have shown mild-to-dramatic differences between them [15, 23, 24]. A fast, final-state π^+ meson "tags" u and $\bar{d}$ quarks (i.e., enhances their contribution to the cross section), while a K^+ tags u and $\bar{s}$. The only difference between the two is the antiquark; if it is causing pronounced changes in Sivers or Boer-Mulders asymmetries, it may be indicative of antiquark OAM. (Alternative explanations, such as higher-twist effects, also exist.) Second, Wakamatsu [25] has confronted the baffling negative sign of $L_u - L_d$ from lattice QCD by calculating L_u and L_d in the chiral quark soliton model, using both the Jaffe and Ji definitions. The paper shows not only the stark difference between the two definitions, but also separates the sea and valence quark contributions. In both definitions, the $\bar{u}$ and $\bar{d}$ antiquarks are the *dominant* players, and in the Jaffe definition, are *entirely* responsible for the negative sign of this quantity. Third, Liu [26] has for the first time succeeded in including disconnected diagrams in a lattice calculation of L. He finds the same: the sea quarks carry as much or more OAM as the valence quarks. Finally, we return to the meson cloud picture. Its orbiting cloud of $L = 1$ pions gives as much OAM to the antiquarks as to the quarks.

1.4 Polarized Drell-Yan: The Missing Spin Program

If we are to resolve the puzzle of quark spin in general and quark OAM in particular, *it is vital to make a direct measurement of the Sivers distribution for antiquarks*. The only process with which this can be cleanly accomplished is Drell-Yan, with its innate sensitivity to antiquarks. (We note that W-production cannot be used in this endeavour as the unobserved neutrino blurs the final-state azimuthal distributions.

The need for a spin-dependent Drell-Yan program has become an urgent priority for the hadron-structure community world-wide. The three processes depicted in Fig. 1 are the only ones where the TMD formalism has been theoretically shown to yield universal functions: PDFs and fragmentation functions that are process-independent. Of the three, only Drell-Yan has not yet been explored with polarized beams and/or targets. It is the missing component in the ultimate goal of a global analysis of TMD-related data. The crucial nature of this missing spin program arises from three facts: the innate sensitivity of Drell-Yan to antiquarks, its freedom from fragmentation functions, and the unique possibility it affords to **test the TMD formalism**. This latter point leads us to the crux of the present proposal.

1.5 This Proposal: the Sivers Sign Change

In the previous sections, we have framed the context in which a polarized Drell-Yan experiment would be placed, and described its crucial place in the spin puzzle. We now turn to the specific motivation for this proposal.

Our proposal is to polarize the Fermilab proton beam and measure spin-dependent Drell-Yan scattering from unpolarized hydrogen and deuterium targets. For Drell-Yan kinematics, $x_f \approx x_b - x_t$, where x_b and x_t are the longitudinal momentum fractions of the annihilated quarks from the beam and target, respectively. As with E-906/SeaQuest, E-866, and their predecessor experiments, the high x_b values selected by the forward $x_f > 0$ spectrometer mean that the partons from the beam will almost certainly be quarks, with the antiquark coming from the target. Taking u-quark dominance into consideration (due to the charge-squared weighting of the cross section and the preponderance of up quarks in the proton at high x), the measurement will be heavily dominated by valence up quarks from the polarized proton beam. The proposed measurement will thus be sensitive to Sivers function for up quarks, $f_{1T}^{\perp,u}(x, \mathbf{k}_T^2)$, times the familiar unpolarized PDF for anti-up quarks, $\bar{u}(x)$.

Given the unique access to sea quarks afforded by the Drell-Yan process, the reader may wonder why this proposal aims to measure the Sivers function for *valence* quarks, and valence *up* quarks at that – the flavor most precisely constrained by SIDIS data from HERMES and COMPASS.

The goal of this first spin-dependent Drell-Yan measurement is exactly to compare Drell-Yan and SIDIS, in order to test the 10-year-old prediction of a **sign change in the Sivers function** from SIDIS to Drell-Yan. Given the theoretical definition of the Sivers function [27], this sign change follows directly from field theory and CPT invariance [28]. Observing the sign change is essential to our interpretation of present and future TMD data in terms of angular momentum and spin. The sign change also offers a rigorous test of QCD in the non-perturbative regime – a rare thing indeed. Observation of the Sivers sign change is one of the DOE milestones for nuclear physics and is the first step for any spin-dependent Drell-Yan program [29].

Beyond the verification of the TMD framework and the tantalizing access it affords to OAM in the proton, there is rich physics behind the Sivers sign change itself. This physics lies in the definition of the Sivers function. The function was first proposed as a possible explanation of the "E-704 effect": the large left-right analyzing power observed in inclusive pion production from a transversely polarized proton beam of 200 GeV incident on a beryllium target. The polarized beam at FNAL-E-704 was a tertiary beam obtained from the production and subsequent decay of hyperons. (Its intensity was thus far below that required for Drell-Yan measurements.) As has happened repeatedly when spin degrees of freedom are introduced for the first time in experimental channels, new effects were observed at E-704 that provoked rich new areas of study. The measured analyzing power was $A_N \propto \vec{S}_{\text{beam}} \cdot (\vec{p}_{\text{beam}} \times \vec{p}_{\text{pion}})$. This single-spin asymmetry is odd under so-called "naive time-reversal", the operation that reverses all vectors and pseudo-vectors but does not exchange initial and final states. The only way to produce such an observable with a T-even interaction is via the *interference* of T-even amplitudes. The interfering amplitudes must have different helicity structures – one spin-flip and one non-spin-flip amplitude are required – and they must differ by a non-trivial phase. Both of these requirements are greatly suppressed in the perturbative hard-scattering subprocess, so the source of the E-704 effect must be soft physics [30]: an interference in either the initial or final state. The original Sivers idea was of an initial-state interference [31]; a complementary proposal from Collins suggested a spin-orbit effect within the fragmentation process [32].

The breakthrough that led to our modern understanding of the E-704 analyzing power occurred many years later when the HERMES collaboration measured pion single-spin asymmetries for the first time in *deep-inelastic scattering*, i.e., using a lepton rather than proton beam [33]. Unlike inclusive $pp \to \pi$, the SIDIS process $ep \to e'\pi$ allows complete kinematic determination of one side of the hard scattering diagram and involves two distinct scattering planes (as do all three processes in Fig. 1). With this additional control,

HERMES was able to separate single-spin effects arising from initial- and final-state interactions [34]. An electron beam interacts much more weakly than a hadron beam. It was widely assumed that initial-state interactions would be excluded in SIDIS, thereby isolating the final-state "Collins mechanism", but the data showed otherwise: both initial- and final-state effects were found to be sizable. The explanation was provided in 2002 by Brodsky, Hwang, and Schmidt [6]. They revisited the QCD factorization theorems and discovered that previously-neglected *gauge-links* between the struck quark and target remnant – soft gluon reinteractions necessary for gauge invariance – had to be included in the very definition of the parton distribution functions. Their paper presented a proof-of-principle calculation showing how a naive-T-odd distribution function could be generated at leading twist, and therefore observable in lepton SIDIS at high Q^2: by interfering two diagrams within the PDF's definition, one with no gauge-link rescattering and an $L = 0$ quark, and one with a single gluon exchanged and an $L = 1$ quark.

This PDF is what is now called the Sivers function, $f_{1T}^{\perp,q}$. Its definition and its very existence at leading twist are intimately related to gauge invariance and our understanding of QCD as a gauge theory. Its universality has been demonstrated – to within a sign – only for SIDIS and Drell-Yan (Fig. 1). The sign change arises from the different topology of the gauge links in these two hard-scattering processes (Fig. 3). In the SIDIS case, the reinteraction is attractive as it occurs between the struck quark and the target remnant. For the Drell-Yan case, the reinteraction is repulsive as it connects the parton from the beam to the remnant from the target (and vice versa). As Dennis Sivers has put it, the Sivers function and its sign change teach us about the **gauge structure of QCD** itself.

Testing the Sivers sign change is vital to the ongoing study of TMDs. It is the inevitable first step for any Drell-Yan spin program and is the key goals of this proposal. By polarizing the Main Injector beam, Fermilab will be able to continue its long and distinguished history of landmark Drell-Yan measurements and take the first step toward becoming the site of the missing piece of the global spin program.

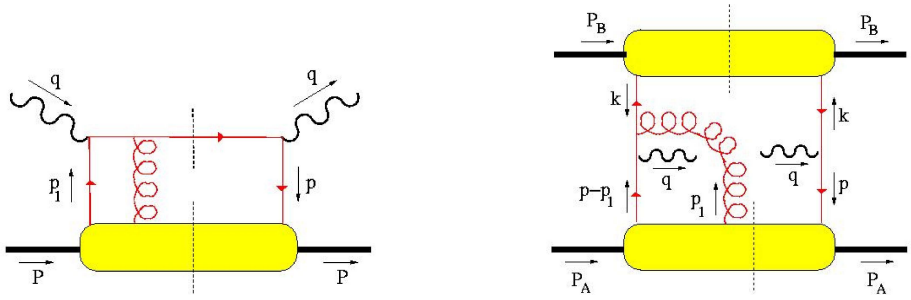

Figure 3: Gauge link topology of the one-gluon exchange forward scattering amplitudes involved in the Sivers function in the (a) semi-inclusive DIS and (b) Drell-Yan scattering processes.

2 Drell-Yan Dimuon Production

The study of the Sivers mechanism in the Drell-Yan process is of particular interest to experimentally verify the fundamental QCD prediction of a sign change between the Sivers function in the Drell-Yan and deep-inelastic scattering processes. As motivated in Section 1.5, this sign change is a consequence of the

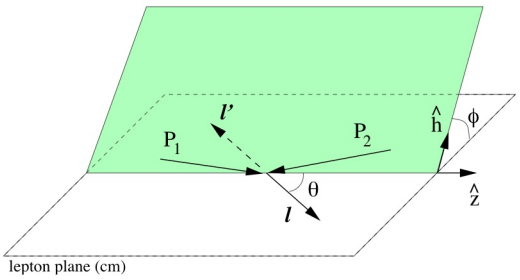

Figure 4: Illustration of the Collins-Soper angles θ and ϕ defined in the $\mu^+\mu^-$ center-of-mass system.

naive-time-reversal-odd property of the Sivers function. This property provides a mechanism to explain the otherwise puzzling observation of the single-spin asymmetries (SSA) for those processes. In this section, it is described how Fourier amplitudes of single-spin asymmetries that arise from the Sivers function can be extracted from a measurement of the angular dependence of the Drell-Yan process involving a transversely polarized beam.

2.1 Single-spin asymmetries

Single-spin asymmetries are observed in various processes over a wide range in the center-of-mass energy [35]. A prominent example is the *E-704 effect* seen at Fermilab: The E-581/E-704 collaboration reported large single-spin asymmetries in the inclusive measurement of pions produced in the collision of transversely polarized (anti)protons with an unpolarized hydrogen target [36, 37]. The single-spin asymmetry of this process, $p^{\Uparrow}p \rightarrow \pi X$, is defined as

$$A_N = \frac{d\sigma^{\Uparrow} - d\sigma^{\Downarrow}}{d\sigma^{\Uparrow} + d\sigma^{\Downarrow}}, \tag{5}$$

where $d\sigma^{\Uparrow(\Downarrow)}$ states the differential cross section for the (anti)proton beam transversely polarized upwards (downwards) w.r.t. the production plane. In the center-of-mass frame, a non-vanishing single-spin asymmetry implies a preference of the produced pions to move left or right w.r.t. to the beam direction. Thus, the single-spin asymmetry A_N is also denoted as left-right asymmetry. The results obtained by the E-581/E-704 collaboration at center-of-mass energies of about 20 GeV were confirmed at center-of-mass energies up to 200 GeV by the STAR and BRAHMS collaboration at RHIC [38, 39].

Single-spin asymmetries involving transversely polarized hadrons are related to the interference of scattering amplitudes with different hadron helicities. This interference is suppressed in hard scattering processes [30], but can be caused by initial- or final-state interactions [6]. The distribution function with the property to induce interactions in the initial or final state are known as naive time reversal odd.

2.1.1 The angular dependence of the Drell-Yan cross section

When studying the angular dependence of the proton induced Drell-Yan process, $p^{\Uparrow}p \to \mu^+\mu^-$, three angles are of relevance: the azimuthal angle ϕ_b of the transverse spin orientation $\mathbf{S}_T$ of the beam (determined in the target rest frame) and the polar and azimuthal angles θ and ϕ of the dimuon pair (determined in the Collins-Soper frame [40], i.e. the dimuon center-of-mass system). The definition of the angles θ and ϕ is shown in Fig. 4. In the one-photon approximation, the differential cross section through the orientation $d\Omega$ of the dimuon pair can be decomposed in a model-independent way [41] such that

$$\begin{aligned}
\frac{d\sigma}{d^4q\,d\Omega} \;=\; & \frac{\alpha^2}{4q^2\sqrt{(P_b\cdot P_t)^2 - M_p^2}} \\
& \Big\{ \quad \Big[\left(1+\cos^2\theta\right) F_{\mathrm{UU}}^{1} + \left(1-\cos^2\theta\right) F_{\mathrm{UU}}^{2} \\
& \qquad + \sin 2\theta \cos\phi\, F_{\mathrm{UU}}^{\cos\phi} + \sin^2\theta \cos 2\phi\, F_{\mathrm{UU}}^{\cos 2\phi} \Big] \\
& + \quad S_L \quad \Big[\sin 2\theta \sin\phi\, F_{\mathrm{LU}}^{\sin\phi} + \sin^2\theta \sin 2\phi\, F_{\mathrm{LU}}^{\sin 2\phi} \Big] \\
& + \quad S_T \quad \Big[\sin\phi_b \Big(\left(1+\cos^2\theta\right) F_{\mathrm{TU}}^{1} + \left(1-\cos^2\theta\right) F_{\mathrm{TU}}^{2} \\
& \qquad + \sin 2\theta \cos\phi\, F_{\mathrm{TU}}^{\cos\phi} + \sin^2\theta \cos 2\phi\, F_{\mathrm{TU}}^{\cos 2\phi} \Big) \\
& \qquad + \cos\phi_b \left(\sin 2\theta \sin\phi\, F_{\mathrm{TU}}^{\sin\phi} + \sin^2\theta \sin 2\phi\, F_{\mathrm{TU}}^{\cos 2\phi} \right) \Big] \\
& \Big\}.
\end{aligned} \tag{6}$$

Here, only partial cross sections are included where the polarization component S_T (S_L) of the beam is transverse (longitudinal) to the direction of the virtual photon. The structure functions $F(P_b\cdot q, P_t\cdot q, q\cdot q)$ depend on three independent Lorentz scalars calculated from the beam, target and virtual photon momenta P_b, P_t and q. Their first and second subscripts indicate, respectively, the beam and target polarizations ((U)npolarized, (L)ongitudinally polarized, (T)ransversely polarized). The related azimuthal modulation is given in a superscript. The Sivers mechanism manifests itself in a $\sin\phi_b\left(1+\cos^2\theta\right)$ modulation in the cross section.

For small transverse momentum of the virtual photon, $q_T \ll q$, the process-dependent structure functions can be interpreted as convolution in transverse momentum space of the universal quark and antiquark distributions of beam and target. At leading twist accuracy and at leading order in α_S, the structure function F_{TU}^{1} provides a signal for the Sivers TMD $f_{1T}^{\perp}$ in conjunction with the well-known polarization-averaged PDF $\bar{f}_1$ of antiquarks such that

$$F_{\mathrm{TU}}^{1} = -\mathcal{C}\left[\frac{\mathbf{q}_T\cdot\mathbf{k}_{T,b}}{q_T M_p} f_{1T}^{\perp}\left(x_b, \mathbf{k}_{T,b}^2\right) \bar{f}_1\left(x_t, \mathbf{k}_{T,t}^2\right) \right]. \tag{7}$$

Here, the convolution over the intrinsic transverse momenta $\mathbf{k}_T$ of the quark and antiquark is represented by the symbol $\mathcal{C}$. Recent Lattice QCD calculations are providing information on the $\mathbf{k}_T$ dependence [42, 43]. These results are in agreement with a phenomenological analysis of deep-inelastic scattering and Drell- Yan measurements [44].

The Sivers function can be experimentally constrained by a measurement of the angular distribution of dimuon pairs produced in the Drell-Yan process with a transversely polarized beam. The structure function F_{TU}^{1} is revealed in a $\sin\phi_b\left(1+\cos^2\theta\right)$ signature. A signal for F_{TU}^{1} can be extracted in a Fourier analysis of the SSA A_N. The corresponding Fourier component or asymmetry amplitude, $A_{\mathrm{TU}}^{\sin\phi_b}$, is given by

$$A_{\mathrm{TU}}^{\sin\phi_b} = \frac{F_{\mathrm{TU}}^{1}}{F_{\mathrm{UU}}^{1}}, \tag{8}$$

where the structure function F_{UU}^{1} can be interpreted as convolution in transverse momentum space of the polarization averaged PDF for quarks and for antiquarks.

2.2 Kinematic Coverage and Spectrometer Acceptance

The kinematic coverage and spectrometer acceptance of the proposed measurement are similar to those of the E-906/SeaQuest experiment. Assuming the 120 GeV polarized beam of the Main Injector impinging on the E-906/SeaQuest cryogenic targets, the E-906/SeaQuest spectrometer accommodates a large coverage in x, *i.e.* $x_b = 0.35 - 0.85$, covering the valence quark region, and $x_t = 0.1 - 0.45$ covering the sea quark region. For the invariant dimuon mass range of $4.2 < M < 8.5\,\mathrm{GeV}$, the acceptance of the proposed measurement is shown in Fig. 5.

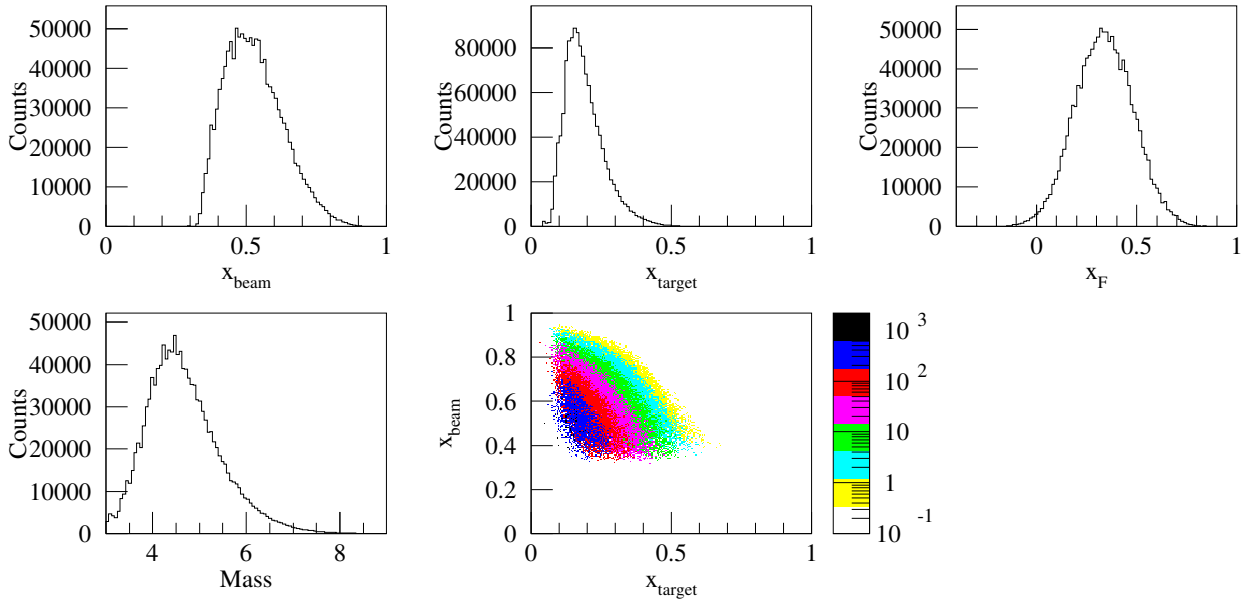

Figure 5: E-906/SeaQuest spectrometer acceptance normalized to total number of protons on the target requested (3.2×10^{18}) for the dimuon mass range of $4.2 < M < 8.5\,\mathrm{GeV}$.

2.3 Event rates and projected statistical precision

In this section, we present the estimation of the luminosity at the Main Injector with a 120 GeV polarized proton beam, the expected Drell-Yan event rates, and the statistical precision that can be achieved in a 2-year long run with a beam polarization of 70%. The analysis is limited to the invariant mass region $4.2 < M < 8.5$ GeV to avoid the region where the J/ψ and Υ, respectively, are prominent. The projected statistical precision in the Sivers asymmetry is based on a Monte Carlo code employed by E-866 and tuned for E-906, and compared to a theoretical prediction for the 120 GeV polarized proton beam in the Main Injector.

The expected instantaneous luminosity, L, on a fixed target can be expressed as

$$L = N_p \cdot I, \tag{9}$$

where N_p is the number of protons/cm^2, and I is the beam current, in number of protons/s. For the liquid hydrogen target (LH_2) used in E-906/SeaQuest, with its density $\rho = 0.0678$ g/cm^3 and length $l = 50.8$ cm

$$N_p = l \cdot \rho \cdot N_A = 2.1 \times 10^{24}/\mathrm{cm}^2, \tag{10}$$

where N_A is the Avogadro's number. Based on a study submitted to the Fermilab directors in August 2011 [45], it is expected that an ion source that produces 1 mA at the source can deliver up to 150 nA (9.5×10^{11} p/s) average beam current to the experiment, using 100% of the available beam time. For details see Section 3.2.

There are however two important limitations to running a polarized Drell-Yan experiment with 150 nA of average beam current. First, the liquid targets for E-906/SeaQuest are designed for average beam currents of about 80 nA, *i.e.* three times the beam current foreseen for E-906/SeaQuest. More importantly, current priorities at Fermilab do not allow to divert more than 10% of the available beam time from the neutrino program. Thus, assuming an average polarized beam current of 15 nA (0.95×10^{11} p/s), a polarized beam luminosity L_p of

$$L_p = N_p \cdot I_p = 2.0 \times 10^{35}/\mathrm{cm}^2/\mathrm{s} \tag{11}$$

can be obtained.

2.3.1 Expected rates of Drell-Yan events

The Drell-Yan event rate per day is estimated according to the expression

$$R = N_{\mathrm{DY}} \cdot \varepsilon_{exp}\,, \tag{12}$$

where N_{DY} is the number of Drell-Yan events estimated from the Monte Carlo simulation and ε_{exp} is the experimental efficiency which includes the spectrometer as well as the accelerator efficiency. The experimental efficiency is estimated to be 0.5 based on the performance of E-906/SeaQuest. In the Monte Carlo simulation, R is estimated using a luminosity of $2.0 \times 10^{35}/\mathrm{cm}^2/\mathrm{s}$ as well as the spill information, various efficiencies and the spectrometer acceptance listed in Table 2. The expected number of Drell-Yan events as a function of x_f are shown in Table 3 for the dimuon mass range of $4.2 < M < 8.5$ GeV, assuming 3.2×10^{18}

protons on target.

Table 1: Various relevant experimental factors used in the Monte Carlo simulation for the Drell -Yan rate estimation. Note that ε_r is the reconstruction efficiency, ε_t is the trigger efficiency, t_{spill} is the time of one spill and n_{spill} is the maximum number of spills per minute.

l_{H_2}	50.8 cm
ρ_{H_2}	0.0678 g/cm^3
I_p	9.5×10^{10} p/s = 15 nA
L	2×10^{35} cm^{-2}s^{-1}
Ω	0.02
ε_r	0.5
ε_t	0.8
t_{spill}	2 s
n_{spill}	3 /min
ε_{exp}	0.5

Table 2: The number of Drell-Yan events estimated per day for the dimuon invariant mass range $4.2 < M < 8.5$ GeV assuming an experimental efficiency (ε_{exp}) of 0.5.

Invariant Mass (GeV)	R (/day)
$4.2 < M < 8.5$	1,865

2.3.2 Expected statistical precision and comparison to theoretical predictions

In this subsection, experimental asymmetries are presented based on Monte Carlo simulations of the E-906/SeaQuest spectrometer, and on a prediction of the Sivers asymmetry by Anselmino and his group [46] as a function of $x_f(\approx x_b - x_t)$ for a 120 GeV polarized beam on an unpolarized hydrogen target. The Sivers asymmetry prediction[1], shown in Fig. 6, is based on a fit to existing semi-inclusive DIS data, i.e., $lp^{\Uparrow} \rightarrow l'hX$ from HERMES [15, 47, 48] and COMPASS [16, 49] for a dimuon mass range of $4.2 < M < 8.5$ GeV. The red line indicates the prediction for the Sivers asymmetry, and the gray shaded area represents the $\sqrt{20}$-sigma error band.[2]

In the Monte Carlo generators used for E-906/SeaQuest, polarization-dependent effects are not simulated. The Sivers mechanism is incorporated in the available Monte Carlo simulations by assigning the beam spin orientation of each generated event randomly according to the polarization-dependent cross section $\sigma_{\text{TU}}^{\Uparrow(\Downarrow)}$. The cross section contribution $\sigma_{\text{TU}}^{\Uparrow}$ for beam spin orientation "$\Uparrow$" is related to the beam-polarization

[1] A word about reference frames and notation: Contrary to the usual study of the angular dependence of Drell-Yan processes, Anselmino chose the hadronic c.m. system instead of the Collins-Soper frame. Furthermore, his notation for the Sivers SSA is $A_N^{\sin(\phi_\gamma-\phi_S)}$ in contrast to the notation of $A_{UT}^{\sin(\phi-\phi_S)}$ commonly used in SIDIS.

[2] The χ^2 analysis and the statistical uncertainty bands are discussed in the Appendix of Ref. [17]. The error band corresponds to a $\Delta\chi^2 = 20$.

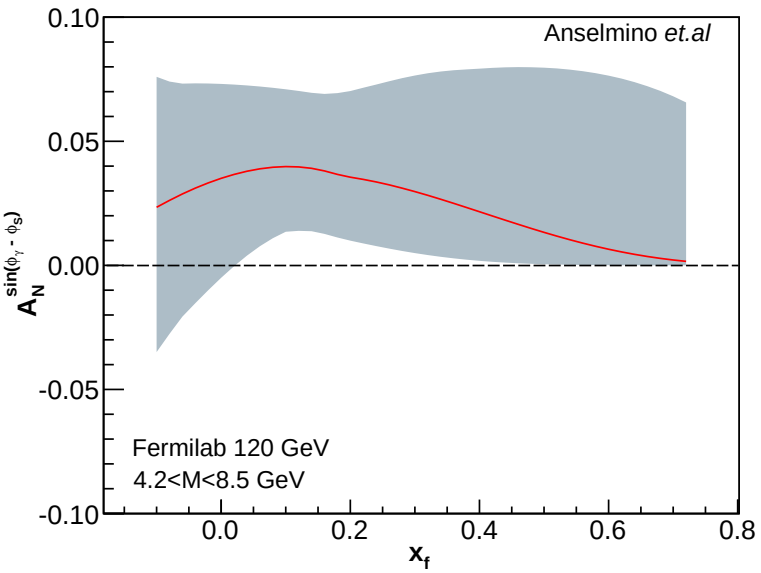

Figure 6: Sivers asymmetry, $A_N^{\sin(\phi_\gamma - \phi_S)}$, as a function of x_f for a polarized Drell-Yan experiment at the Fermilab Main Injector [46]. The red line indicates the prediction for the Sivers SSA, and the gray shaded area represents the $\sqrt{20}$-sigma error band.

dependent SSA A_{TU} via

$$\sigma_{\mathrm{TU}}^{\Uparrow} = \sigma_{\mathrm{UU}}(1 + A_{\mathrm{TU}}). \tag{13}$$

Using the SSA prediction by Anselmino for A_{TU}, the polarization-dependent cross section can be estimated for the generated events: If a random number ρ ($\rho \in [0;1]$) does (not) fulfill the condition

$$\rho < \frac{1}{2}(1 + A_{\mathrm{TU}}), \tag{14}$$

then beam spin orientation "$\Uparrow$" ("$\Downarrow$") is assigned. This method allows for a simulation of the Sivers analysis at the proposed, polarized Drell-Yan experiment, as shown in Fig. 7 and Table 3.

2.4 Comparison to Competition

There are plans for a wide variety of experiments around the globe that aim to measure polarized Drell-Yan either with a polarized beam or a polarized target (see Table 4). COMPASS at CERN, Panda at GSI, and an internal target program at RHIC (BNL) plan to perform fixed target experiments with either pion, proton or anti-proton beams, whereas PAX at GSI, and NICA at JINR plan collider experiments with polarized proton beams. The fixed target experiments typically provide higher luminosity, and the collider experiments tend to run at higher center of mass energy, s. NICA and the polarized Drell-Yan programs at RHIC will be sensitive to the interaction between valence quarks and sea antiquarks. PAX and COMPASS plan to measure the interaction between valence quarks and valence antiquarks, and are not sensitive to sea antiquarks. And

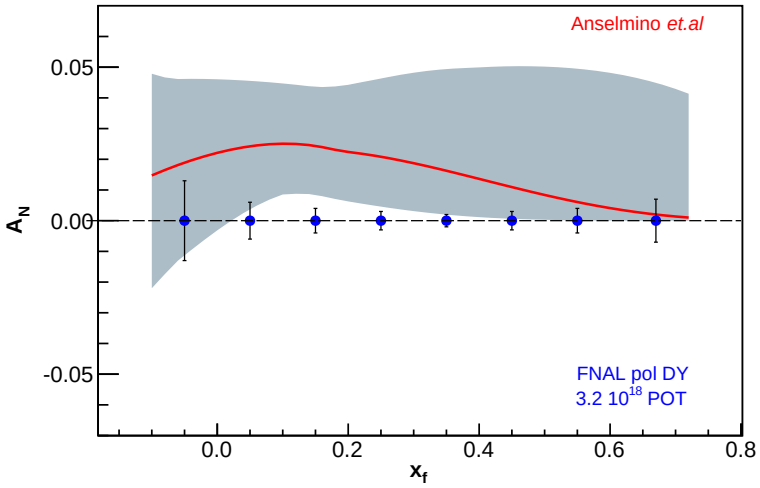

Figure 7: Single spin asymmetry A_N as a function of x_f. The SSA A_N (red line) is related to the Sivers SSA amplitude by $A_N = \frac{2}{\pi} A_{\mathrm{TU}}^{\sin\phi_b}$. The expected statistical uncertainties (blue solid circles) for a 70% polarized beam on an unpolarized target and 3.2×10^{18} protons on target are (arbitrarily) plotted on the zeroline.

Panda is designed to study J/Ψ formation rather than Drell-Yan physics due to the low antiproton beam energy. At present, only the COMPASS experiment is scheduled to run in the near future. COMPASS is scheduled to take data in 2014 for one year and expects to measure the sign of the Sivers function in the same kinematics as semi-inclusive DIS[3] with a statistical precision of $\delta A_N/A_N$ of 1%–2%. As shown in Fig. 7, a polarized Drell-Yan experiment such as E-906/SeaQuest is needed, however, to measure the sign, the magnitude, and possibly the shape of the Sivers function with sufficiently high precision.

The big attraction for a polarized Drell-Yan program at the Fermilab Main Injector is the high luminosity in combination with a spectrometer and a hydrogen target that are well-understood, fully functioning, and optimized for Drell-Yan at the end of data collection for the E-906/SeaQuest experiment (estimated to be in early 2015). Furthermore, the E-906/SeaQuest spectrometer accommodates a large coverage in parton momentum fraction x, *i.e.* $x_b = 0.35 - 0.85$ covering the valence quark region, and $x_t = 0.1 - 0.45$ covering the sea quark region. Although the Sivers function can be measured for both the valence quarks or the sea quarks, valence quarks constrain the SIDIS data from HERMES and COMPASS much more than the sea quarks [17, 50]. Thus, using a polarized beam promises to be a substantial advantage over a polarized target.

The combination of high luminosity, large x-coverage and a high-intensity polarized beam makes Fermilab arguably the best place to measure single-spin asymmetries in polarized Drell-Yan scattering with high precision. It would allow for the first time to perform a measurement of the sign, the magnitude, and the shape of the Sivers function with sufficient precision to verify this fundamental prediction of QCD conclusively.

[3]Note, COMPASS will measure A_N in one x_f-bin centered at $x_f = 0.2$ in the invariant mass region $4 < M < 9$ GeV.

Table 3: Expected number of Drell-Yan events, $N_{\rm DY}$, for each x_f bin considered. The statistical precision for the measured asymmetries, δA, for invariant mass region $4.2 < M < 8.5$ GeV is also shown. The total number of protons on target is assumed to be 3.2×10^{18}.

x_f	$N_{\rm DY}(x_f)$	$\delta A(x_f)$
$-0.2 < x_f < 0.0$	11,700	0.013
$0.0 < x_f < 0.1$	50,300	0.006
$0.1 < x_f < 0.2$	163,100	0.004
$0.2 < x_f < 0.3$	293,200	0.003
$0.3 < x_f < 0.4$	342,900	0.002
$0.4 < x_f < 0.5$	263,200	0.003
$0.5 < x_f < 0.6$	124,700	0.004
$0.6 < x_f < 0.8$	45,500	0.007

3 Experimental Apparatus

The proposed measurements will make use of the existing SeaQuest Spectrometer located in the NM4 (formerly KTeV) enclosure. This spectrometer is presently being used by the E-906/SeaQuest [57] experiment for unpolarized Drell-Yan measurements on hydrogen, deuterium and a variety of nuclear targets, but will be available on the time scale of this project. The significant effort and cost in mounting this experiment will be the development of an extracted, polarized beam from the Fermilab Main Injector. This section discusses the E-906/SeaQuest spectrometer and its performance, followed by a discussion of the modifications to produce a polarized proton beam at the Fermilab Main Injector.

3.1 The E-906/SeaQuest Spectrometer

The DOE/Office of Nuclear Physics and Fermilab have already made a substantial investment in the SeaQuest spectrometer and the beam line. The proposed measurements will make use of both. The spectrometer will require no modifications beyond those envisioned to take place in the 2012-13 shutdown. The spectrometer is shown schematically in Fig. 8.

The basic concept behind the spectrometer is that the first magnet serves triple purpose: it focuses oppositely signed muon pairs into the spectrometer; it contains the beam dump for the primary proton beam; and, at the same time, serves as an absorber for all non-muons produced in beam target and beam-dump collisions. This magnet is constructed out of solid iron and is known as FMag by the experiment. This magnet was constructed by repurposing one set of coils from the SM3 magnet and iron from the SM12 magnet. Both of these magnets were used by previous Fermilab Drell-Yan experiments. Because of the extremely high particle density between the targets and FMag, there are no detector elements places in this region. While the iron in FMag does an excellent job of preventing non-muons from reaching the rest of the spectrometer, the multiple scattering and energy loss that the muons undergo while traversing approximately 4.9 m of iron is substantial and represents the largest uncertainty in reconstructing the events. From Monte Carlo estimates, we expect a mass resolution of $\sigma_M \approx 250$ MeV at the J/ψ.

Table 4: Planned polarized Drell-Yan experiments. x_b and x_t are the parton momentum fractions in the beam and target, respectively.

experiment		particles	energy	x_b or x_t	luminosity	timeline
COMPASS (CERN)	[51]	$\pi^{\pm} + p^{\uparrow}$	160 GeV $\sqrt{s}$ = 17.4 GeV	$x_t = 0.2 - 0.3$	$1 \times 10^{32}\ cm^{-2}s^{-1}$	2014
PAX (GSI)	[52]	$p^{\uparrow} + \overline{p}$	collider $\sqrt{s}$ = 14 GeV	$x_b = 0.1 - 0.9$	$2 \times 10^{30}\ cm^{-2}s^{-1}$	>2017
PANDA (GSI)	[53]	$\overline{p} + p^{\uparrow}$	15 GeV $\sqrt{s}$ = 5.5 GeV	$x_t = 0.2 - 0.4$	$2 \times 10^{32}\ cm^{-2}s^{-1}$	>2016
NICA (JINR)	[54]	$p^{\uparrow} + p$	collider $\sqrt{s}$ = 20 GeV	$x_b = 0.1 - 0.8$	$1 \times 10^{30}\ cm^{-2}s^{-1}$	>2014
PHENIX (BNL)	[55]	$p^{\uparrow} + p$	collider $\sqrt{s}$ = 200 GeV	$x_b = 0.05 - 0.1$	$2 \times 10^{32}\ cm^{-2}s^{-1}$	>2018
RHIC internal target phase-1	[56]	$p^{\uparrow} + p$	250 GeV $\sqrt{s}$ = 22 GeV	$x_b = 0.25 - 0.4$	$2 \times 10^{33}\ cm^{-2}s^{-1}$	>2015
RHIC internal target phase-2	[56]	$p^{\uparrow} + p$	250 GeV $\sqrt{s}$ = 22 GeV	$x_b = 0.25 - 0.4$	$3 \times 10^{34}\ cm^{-2}s^{-1}$	>2018
E-906/SeaQuest (FNAL)	[57]	$p + p$	120 GeV $\sqrt{s}$ = 15 GeV	$x_b = 0.35 - 0.85$ $x_t = 0.1 - 0.45$	$2 \times 10^{35}\ cm^{-2}s^{-1}$	2012
pol. SeaQuest ‡ (FNAL)		$p^{\uparrow} + p$	120 GeV $\sqrt{s}$ = 15 GeV	$x_b = 0.35 - 0.85$	$1 \times 10^{36}\ cm^{-2}s^{-1}$	>2015

‡ $L = 1 \times 10^{36}\ cm^{-2}s^{-1}$ (SeaQuest LH_2 target limited), $L = 2 \times 10^{35}\ cm^{-2}s^{-1}$ (10% of MI beam limited)

Downstream of the first magnet are four "stations", numbered from the most upstream station. Each station consists of a set of scintillator hodoscopes and a tracking detector. The detailed dimensions of each station are given in Table 5. The hodoscope arrays at each station allowed the spectrometer to be triggered on specific roads that were preprogrammed, according to Monte Carlo studies, to select high p_T muons. The trigger is discussed in more detail in Section 3.1.1.

A second spectrometer magnet is located between stations (Sts.) 1 and 2. Known as KMag in the E-906/SeaQuest experiment, this magnet was formerly the KTeV spectrometer magnet. The primary function of this magnet is to bend trajectories of the muons that have survived the trip through FMag and thereby provide a momentum measurement.

The target system for E-906/SeaQuest consisted of a liquid hydrogen (LH_2) target, a liquid deuterium (LD_2) target, an empty flask, and four solid targets (Fe, C, W, and "no target"). The entire target system was mounted on a movable table so that the experiment could easily interchange targets between spills. For the proposed measurement, only the liquid targets and empty flask will be used. The LD_2 target was 12% of an interaction length and the LH_2 target was 6.9%. The liquid targets were 50.8 cm long and each contained 2.2 liters. The target flask pressure, which is proportional to the system temperature, is controlled using a set of heaters (resistors) that are served with an AC current regulated through a silicon controlled rectifier. The heater power is adjusted using a feedback loop known as a PID (proportional integral derivative) to keep the flask pressure constant. With a maximum beam intensity of 10^{12} protons per pulse, the expected heat deposit is 5 W over 5 s on the liquid targets, for a total of 25 Joules per spill. Each of the liquid targets was attached to a cooper condenser that was cooled by a stand-alone Cryomech cryocooler. The cryocooler was

Table 5: Summary of the locations, number of elements, orientations, *etc* of the detectors in the SeaQuest spectrometer.

			Station			
			1	2	3	4
Hodoscopes	x	z (cm)	636	1421	1961	2240
		Area ($x \times y$ cm)	161×70	203×121	224×168	305×183
		No. Elements	23	16	16	16
	y	z (cm)	650	1403	–	2135, 2210 (2)
		Area ($x \times y$ cm)	79×140	102×241	–	229×366
		No. Elements	20	19	–	16
			1	2	3-	3+
Tracking		z (cm)	556	1344	1881	1939
		Area ($x \times y$ cm)	101.6×121.9	$233.2(242.6) \times 269.2$	180.0×167.6	232.0×160.0
		Views	x, x', u, u', v, v'	x, x', u, u', v, v'	x, x', u, u', v, v'	x, x', u, u', v, v'
		Stereo Angle	$(\pm 14^\circ)$	$(\pm 14^\circ)$	$(\pm 14^\circ)$	$(\pm 14^\circ)$
		No. Elements	160 (201)	112 (128)	176 (208)	116 (134)
		Wire Spacing (cm)	0.635	2.08 (2.02)	1.02 (0.99)	2.0
Upgrades (in progress)		z (cm)	556	–	1881	–
		Area ($x \times y$ cm)	137.2×152.4	–	232.0×160.0	–
		Views	x, x', u, u', v, v'	–	x, x', u, u', v, v'	–
		Stereo Angle	$(\pm 14^\circ)$	–	$(\pm 14^\circ)$	–
		No. Elements		–	116 (134)	–
		Wire Spacing (cm)	0.500 (0.505)	–	2.0	–

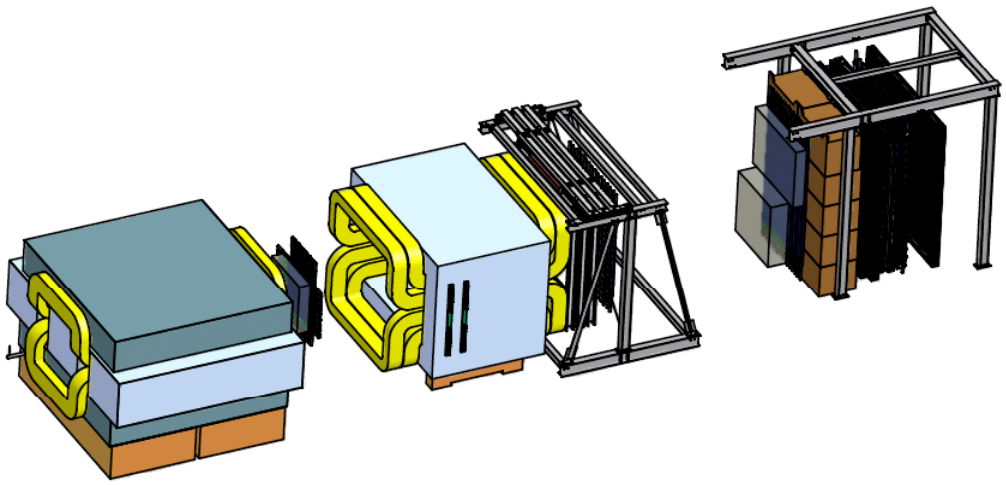

Figure 8: Schematic view of the SeaQuest Spectrometer as it was during the 2012 Commissioning run.

capable of removing 25 W at 20 K. During the commissioning run, a feedback loop was able to adjust the flask pressure such that no observable effects due to the beam heat deposit were seen. The target system operated extremely well during the E-906/SeaQuest commissioning run.

It is worth noting that to keep costs reasonable, many of the detector elements at each station were reused from earlier experiments. For example, the liquid target flasks were originally fabricated for the E-866/NuSea experiment. The hodoscopes in St. 1 and 2 came from the HERMES experiment. The St. 3 and 4 hodoscopes reused photomultiplier tubes and bases from the E-866/NuSea Drell-Yan experiment. The tracking chamber at St. 2 was also from E-866/NuSea, as were the tracking chambers used in the 2012 commissioning run at St. 1 and the lower half of St. 3. The tracking chamber at St. 4 came from a Los Alamos Homeland Security project. For the proposed measurement, we anticipate doing even better by reusing the entire spectrometer!

During the present, 2012-13, shutdown, the SeaQuest collaboration is engaging in several upgrades, which originally were in the baseline spectrometer, but were delayed due to other constraints. These include new tracking chambers at St. 1 and St. 3 (lower) for larger acceptance and, at St. 1 better rate capabilities. In addition, the SeaQuest collaboration is now considering modifications to the St. 1 hodoscope photomultiplier bases to enhance their instantaneous rate capabilities. All of these upgrades will be in place before E-906/SeaQuest Run II, starting in Spring 2013, well before the measurements proposed here will take place.

The overall luminosity normalization is done by calibrating ion chambers in the beam line to a copper foil activation. Based on previous experience with this technique in E-866/NuSea, a systematic uncertainty of $\pm 6.5\%$ is expected [60]. The collaboration is investigating the possibility of installing an Unser beam monitor. With such a device, we estimate that an absolute uncertainty of $\pm 1\%$ can be achieved [61].

For better acceptance in x_b we have chosen to run FMag at 75% of full field for this measurement. This choice involves a trade off between statistical precision and uncertainty in kinematic reconstruction due to the knowledge of the field within the solid iron magnet. With further study in E-906/SeaQuest, the collaboration may further optimize this trade off.

3.1.1 Trigger system

The hardware trigger system will utilize the scintillator hodoscope hits to identify events that are likely to be high-mass dimuon pairs. It will be almost identical to the system designed for and used by E-906/SeaQuest [57]. The main trigger logic pipeline will consist of two levels. The first level will identify patterns of hits that correspond to muon tracks through the spectrometer. The second level will examine the tracks identified in the first level and will output a trigger if the tracks correspond to a desired event type (e.g. high-mass, opposite sign dimuon pair). This setup should allow good rejection of random coincidences as well as selection between various types of real muon tracks. It will allow for hardware-level selection between single-muons, high-mass dimuons, and low-mass dimuons (J/ψ).

The hardware for the main trigger electronics will consist of five VME FPGA (Field Programmable Gate Array) modules. Four of these will be used for Level One. One module will be used for each of the following: tracks in upper-half bend-plane hodoscopes, tracks in the lower-half bend-plane hodoscopes, tracks in the upper-half non-bend-plane hodoscopes, and tracks in the lower-half non-bend-plane hodoscopes. These modules will utilize a look-up-table style of logic. Monte Carlo generated data will be used to fill the look-up-table with hit combinations. Each module will require a four-fold coincidence in order to send a track to the Level Two module.

Each of these will output information about the identified tracks to the fifth FPGA module, Level Two. The Level Two module will combine the tracks from Level One to decide how to classify the event. Five output triggers from Level Two will be accepted by the Data-Acquisition System. These five triggers will likely include

1. High-mass opposite-sign dimuon pair (the main trigger),
2. Any-mass opposite-sign dimuon pair,
3. Any single track,
4. Same-sign dimuon pair, and
5. Single-Track in the non-bend-plane.

All trigger types other than the high-mass opposite-sign dimuon pair will be prescaled such that they do not dominate the recorded data. The single-track and same-sign triggers will allow for calculation of expected random coincidence rates in the opposite-sign triggers due to independent single tracks that appear to be Drell-Yan events. Because of the look-up-table design of the Level One logic, the Level Two dimuon triggers will only consider events with at least one track in the bottom half of the spectrometer, and at least one track in the top half of the spectrometer. The non-bend-plane trigger will be used for calculating hodoscope efficiencies. Events from this trigger can be used to calculate the efficiency of the bend-plane hodoscopes, while events from other triggers can be used to calculate the efficiency of the non-bend-plane hodoscopes.

In addition to the FPGA-based trigger system, there will be a parallel NIM-based trigger system, just as in E-906/SeaQuest. The NIM trigger system will be set up similarly to the FPGA system (separating top from bottom, and bend from non-bend), but it will consider any four-fold coincidence valid, as opposed to requiring specific hit combinations. The NIM-based triggers will measure rates of various coincidence requirements as well as provide an independent check on the FPGA-based trigger.

3.2 Polarized Beam at Main Injector

To accelerate polarized protons in the Fermilab Main Injector, modifications are needed [45] in most accelerator stages, as shown in Fig. 9. The major new components needed are a polarized ion source, and two superconducting Siberian snakes in the Main Injector. Recent studies have found though that the superconducting spin rotator in the extraction line that leads to the NM4 experimental area may not be needed.[4]

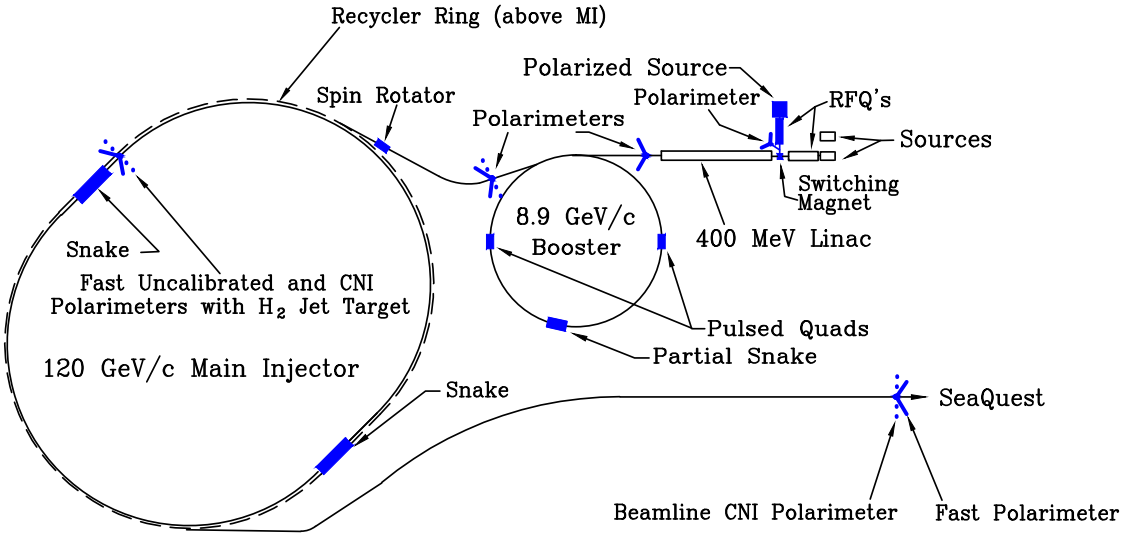

Figure 9: Major components needed (blue symbols) for polarized beam at Fermilab .

Based on the study submitted to the Fermilab directors in August 2011 [45], and experience gathered from current polarized ion sources [58, 59], it is expected that an ion source that produces 1 mA at the source could deliver up to 150 nA (9.5×10^{11} protons/s) average beam current to the experiment, using thirty 2-second cycles and slip stacking in the Main Injector. This assumes that starting with 26 μs long source pulses at a 15 Hz repetition rate going into the linac and injected into the Booster for 12 turns, then 6 Booster pulses injected into the Recycler Ring, followed by 6 more pulses using slip-stacking before injection in the Main Injector ring (with 95% efficiency) will lead to Main Injector pulses of 1.9×10^{12} protons. Using thirty 2-second cycles (1.33-s ramp time plus 0.67-s slow extraction) per minute gives an instantaneous beam intensity of 2.8×10^{12} p/s (=450 nA) and an average beam current of 0.95×10^{12} protons/s (=150 nA).

Fermilab programmatic reasons limit a polarized beam program to 10% of the available beam time. Thus, a running scenario of three 2-second pulses every minute could deliver average beam intensities of 15 nA without impacting the Fermilab neutrino program significantly, and deliver a luminosity of $2.0 \times 10^{35}/\mathrm{cm}^2/\mathrm{s}$. For a 2-year period and an 50% running efficiency, resulting in a total number of 3.2×10^{18} protons on target, about 1.3 million polarized Drell-Yan events could be collected. With two Siberian snakes, each containing four superconducting transverse helical dipole magnets, one could overcome all depolarizing resonances in the Main Injector, and deliver proton beams to the NM4 experimental area with about 75% polarization [45].

[4] Recent studies by the Spin@Fermi Collaboration have found that it may be possibly to eliminate the 120 GeV spin rotator, if the MI beam energy could be reduced from 120.0 GeV to approximately 118.64 GeV. They found that for a $G\gamma \approx 226.74$ the normal spin component at the last magnet before NM4 is near 99%. Eliminating the 120 GeV spin rotator could lead to significant savings.

In this proposal it is assumed, however, that 70% polarization can be obtained on average.

The systematic uncertainty in measuring the beam polarization is expected to be $\Delta P_b/P_b < 5\%$ [62, 63]. Note that the systematic uncertainty in the beam polarization measurement results in a scale uncertainty on the measured asymmetries and extracted Fourier amplitudes, but it does not change the statistical significance of the results.

4 Proposed Schedule

The study of QCD symmetry and the spin-dependent structure of the proton are very exciting and interesting topics. With the acceptance and luminosity of the E-906/SeaQuest spectrometer and the Fermilab Main Injector, the collaboration stands ready to lead the worldwide effort in this exploration with Drell-Yan scattering. As such, the collaboration is adopting a schedule that is as aggressive as possible. While the E-906/SeaQuest experiment will not be completed until 2015, the critical path lies with the polarization of the Main Injector and the funding for this project.

A very aggressive and very schematic schedule is shown in the Gantt charts of Figs. 10 and 11. At this point, the schedule is meant to be schematic and show one possibility for achieving a polarized Drell-Yan experiment at Fermilab. The schedule is divided into three sub-schedules: the Fermilab accelerator complex, the E-906/SeaQuest experiment, the polarization upgrade of the Main Injector, and finally the running of the proposed experiment.

In this schedule, the E-906/SeaQuest experiment will turn on after the 2012-13 shutdown and complete data collection in the first or second quarter of 2015. The accelerator schedule assumes that there are summer shutdowns in the summers of 2014 and 2015, each of approximately 8 weeks in duration. It is during these shutdowns that, with the proper planning and a reasonable funding profile that the installation of most of the components needed in the booster and Main Injector will be installed. The report on polarizing the Main Injector [45] gives more detailed information on these tasks and scheduling; although delayed by a year due to funding considerations. Optimistically, we expect that initial funding for this project may be available in FY14.

5 Requests to Fermilab

In planning for the experiment, most of the tasks related to the spectrometer have been already completed by the E-906/SeaQuest collaboration. There are some areas, however, for which we are specifically requesting that Fermilab take responsibility. Specifically, for the spectrometer, the collaboration requests:

- The continued use of the NM3 and NM4 enclosure to house the new experiment. This area formerly housed the KTeV experiment and now houses the SeaQuest experiment.
- The continued use of the upper level (ground floor) of the SeaQuest Hall as a counting house and workspace. We further request that the part of this area currently being used as tape storage by Computing Division be made available to the collaboration.
- Continue to supply utilities and network connections to both the upstairs area and NM3/4 Hall area.

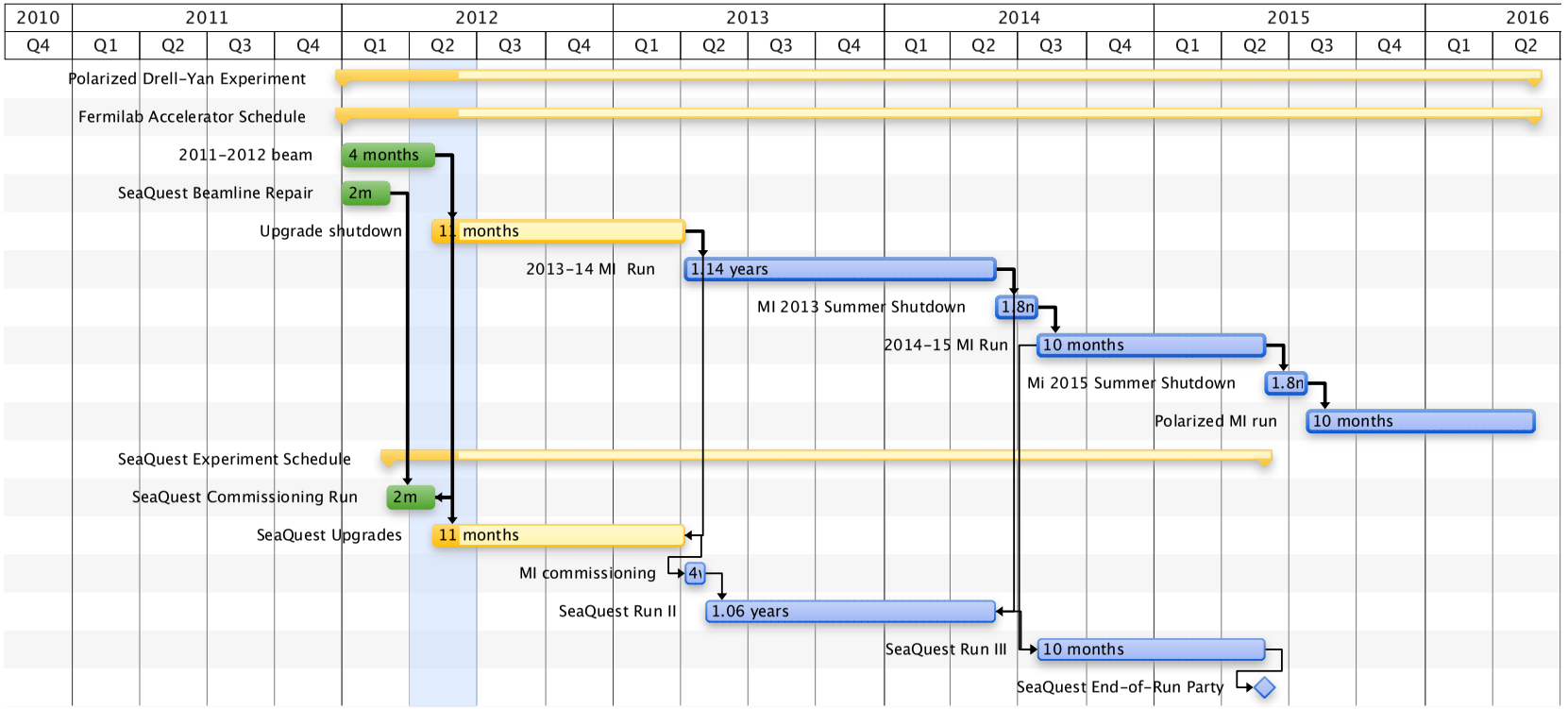

Figure 10: Gantt chart showing the running schedule for E-906/SeaQuest. The SeaQuest experiment will be completed in 2015. With an adequate funding profile, most of the Main Injector work can be done during *hypothetical* summer shutdowns in 2014 and 2015. Naturally, the polarized MI run will extend beyond the timeline shown

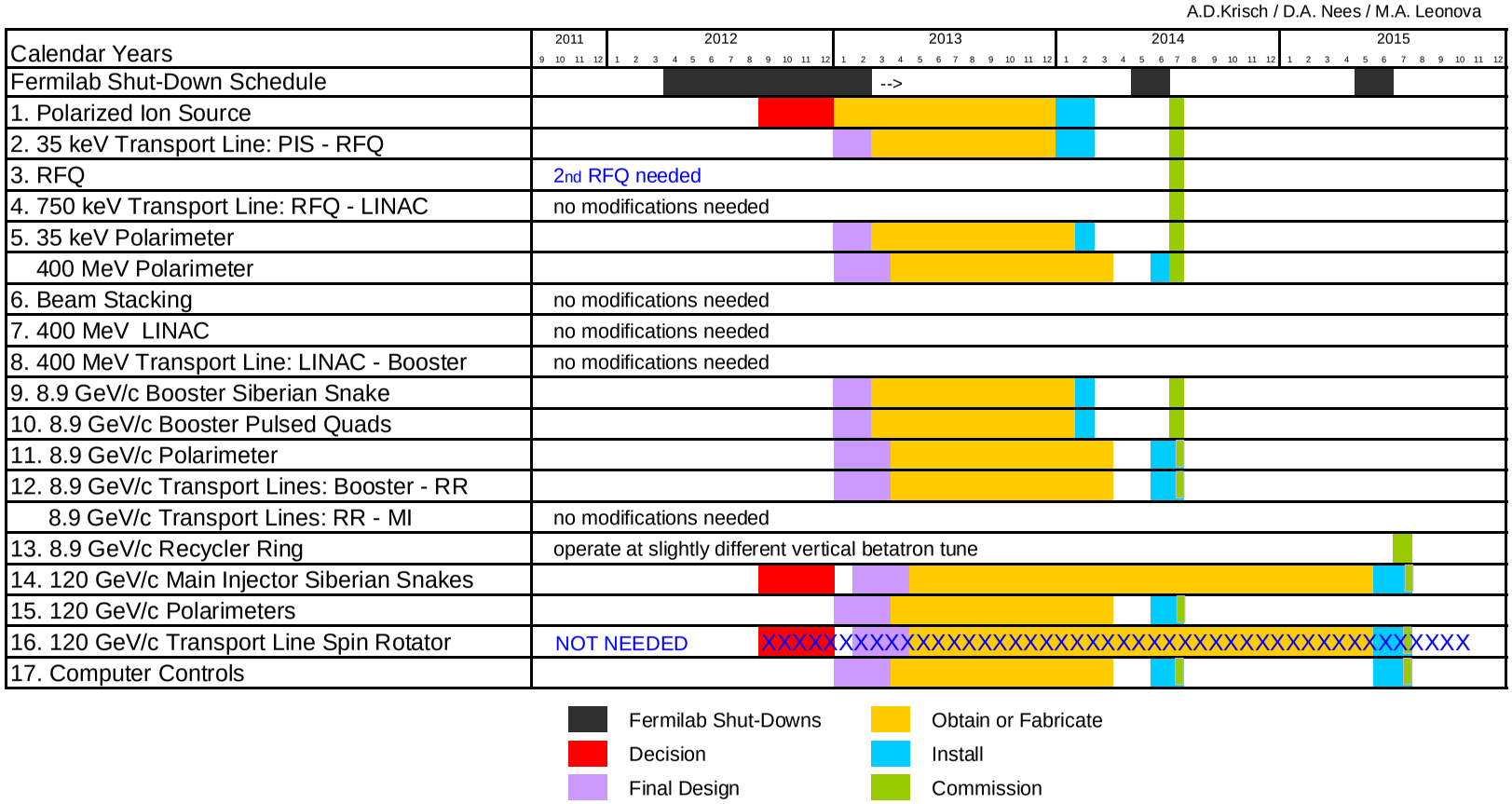

Figure 11: Gantt chart showing a possible schedule for the polarization of the Main Injector. With an adequate funding profile, most of the Main Injector work can be done during *hypothetical* summer shutdowns in 2014 and 2015.

- The continued maintenance of the spectrometer magnets (FMag and KMag) along with their utilities (*e.g.* cooling water and power supplies).
- Provide appropriate radiation shielding, radiation safety interlocks and handle all aspects of radiation safety monitoring. We anticipate that there will be no changes which would require shielding modifications.
- Provide rigging for installation. We anticipate that this will be a minor request, representing only minor modifications to the spectrometer.
- The continued use of the electronics from the PREP equipment pool that is currently assigned to the E-906/SeaQuest experiment.
- Data storage space for Monte Carlo and data produced by the experiment. This is anticipated to be approximately the same as the SeaQuest experiment needs, less than 20 TB.

In general, these represent a request to Fermilab for continued support at approximately the same level that the E-906/SeaQuest Experiment is currently receiving. The collaboration realizes that some parts of these requests may appear vague. As the experiment approaches Fermilab's Stage II approval and the signing of a Memorandum of Understanding with Fermilab, the details of these requests may become more explicit.

With the spectrometer already existing, the heart of this experiment and our request is the extraction of a transversely polarized beam from the Fermilab Main Injector. Specifically we request:

- Provide a beam with a minimum of 70% polarization to the experiment delivered in slow extraction spills for a total of 3.2×10^{18} protons over the duration of the expeirment. One possible scheme to deliver this beam would be for three spills/minute, each consisting of a 1.334 s magnet ramp followed by an 0.667 s extraction. This would comitt only 10% of the available MI to this measurement. The collaboration is, of course, open to other schemes, as may be required to run the accelerator complex efficiently.

Within this is a request for the polarization of the Fermilab Main Injector. The ability to polarize the Main Injector is the subject of a separate study which has been submitted to the Fermilab Directorate [45]. At this time, we are requesting *scientific, Phase I approval for our experiment*. This will allow the collaboration and Fermilab to pursue with DOE the funding necessary to provide such a beam. In the mean time, we further request that

- **Fermilab make every effort to keep the necessary space available in the MI for Siberian snakes, instrumentation and other equipment needed for the polarization of the MI.**

At this time, this is the most important request.

A Funding Model

The measurements we are proposing focus on the nature of QCD by exploring the internal dynamics and symmetries of the proton. Just as the E-906/SeaQuest measurements are of significant interest to both

High Energy Physics and Nuclear Physics, these measurements are as well. Again, in parallel with E-906/SeaQuest, institutions funded out of nominally Nuclear Physics are taking the lead on this experiment, while it will be hosted at the premier High Energy Physics laboratory in the United States. We hope to also follow these parallels with a funding model that invests money from both Nuclear Physics and High Energy Physics through Fermilab into this project.

The measurements proposed in this experiment will leverage the investment in the SeaQuest spectrometer made by DOE/Nuclear Physics (NP), DOE/High Energy Physics (HEP), the US NSF as well as funding agencies in Japan and Taiwan. For E-906/SeaQuest, the primary funding for the spectrometer came from DOE/NP and the NSF with significant and substantial installation support provided by Fermilab. In addition, DOE/NP provided funding for M&S needed for much of the beam line installation with Fermilab providing the effort and additional M&S. The total DOE/NP investment that was transferred to Fermilab was to mount the experiment was approximately $1M, in addition to the DOE/NP investment in the spectrometer itself.

The collaboration is hopeful that a similar model will work for the proposed measurements. We have already been in contact with both DOE/NP and with the Fermilab directorate about these issues. Both were encouraging, but cautious, in the current funding environment. In addition, there was an indication from both that this project would not be funded by only one entity alone, but required the participation of the other as well – possibly in a model similar to that used by E-906/SeaQuest. In addition, it was clear that Fermilab and DOE/NP were interested in the scientific output from this investment. Once Phase I approval is granted to this measurement, we will be able to better pursue cooperative funding between agencies.

References

[1] D. DeFlorian, R. Sassot, M. Stratmann, W. Vogelsang, Phys. Rev. Lett. **101**, 071001 (2008); Phys. Rev. **D80**, 034030 (2009).

[2] P.J. Mulders and R.D. Tangerman, Nucl. Phys. **B461**, 197 (1996).

[3] A. Bacchetta, M. Diehl, K. Goeke, A. Metz, P.J. Mulders, M. Schlegel, JHEP **0702**, 093 (2007).

[4] D.W. Sivers, Phys. Rev. **D41**, 83 (1990); **D43**, 261 (1991).

[5] D. Boer and P.J. Mulders, Phys. Rev. **D57**, 5780 (1998).

[6] S. J. Brodsky, D. S. Hwang, and I. Schmidt, Phys. Lett. **B530**, 99 (2002).

[7] M. Burkardt, Nucl. Phys. **A735**, 185 (2004).

[8] A. Bacchetta and M. Radici, Phys. Rev. Lett. **107**, 212001 (2011).

[9] Z. Liang and T. Meng, Zeit. Phys. **A344**, 171 (1992).

[10] S.V. Bashinsky and R.L. Jaffe, Nucl. Phys. **B536**, 303 (1998).

[11] X. Ji, Phys. Rev. Lett. **78**, 610 (1997).

[12] M. Wakamatsu, J. Phys. Conf. Ser. **295** 012038 (2011); Phys. Rev. **D81**, 114010 (2010); Phys. Rev. **D83**, 014012 (2011).

[13] M. Burkardt and G. Schnell, Phys. Rev. **D74**, 13002 (2006).

[14] P. Hägler *et al.*, Phys. Rev. Lett. **98**, 22 (2007).

[15] (HERMES Collaboration) A. Airapetian *et al.*, Phys. Rev. Lett. **94**, 012002 (2005).

[16] (COMPASS Collaboration) V.Y. Alexakhin *et al.*, Phys. Rev. Lett. **94**, 202002 (2005).

[17] M. Anselmino *et al.*, Eur. Phys. Jour. **A39**, 89 (2009).

[18] N.C.R. Makins, INT Workshop on Orbital Angular Momentum in QCD, http://www.int.washington.edu/talks/WorkShops/int_12_49W/People/Makins_N/Makins.pdf

[19] (FNAL E866/NuSea Collaboration) R.S. Towell *et al.*, Phys. Rev. **D64**, 052002 (2001).

[20] (HERMES Collaboration) A. Airapetian *et al.*, Phys. Rev. **D71**, 012003 (2005); Phys. Rev. Lett. **92**, 012005 (2004).

[21] A.W. Thomas, Phys. Rev. Lett. **101**, 102003 (2008).

[22] (LHPC Collaborations) P. Hägler *et al.*, Phys. Rev. **D77**, 094502 (2008); D. Richards, arXiv:0711.2048.

[23] (HERMES Collaboration) A. Airapetian *et al.*, arXiv:1204.4161 (submitted to Phys. Rev. D).

[24] (BRAHMS Collaboration) I. Arsene *et al.*, Phys. Rev. Lett. **101**, 042001 (2008)

[25] M. Wakamatsu, Eur. Phys. Jour. **A44**, 297 (2010).

[26] K.F. Liu *et al.*, arXiv:1203.6388 [hep-ph].

[27] D. Boer and P.J. Mulders, Phys. Rev. **D57**, 5780 (1998).

[28] J.C. Collins, Phys. Lett. **B536**, 43 (2002).

[29] Report to the nuclear science advisory committee, Aug 2008; Hadronic Physics, Milestone #13, http://science.energy.gov/ /media/np/nsac/pdf/docs/perfmeasevalfinal.pdf

[30] G. L. Kane, J. Pumplin, and W. Repko, Phys. Rev. Lett. **41**, 1689 (1978).

[31] D.W. Sivers, Phys. Rev. **D41**, 83 (1990); Phys. Rev. **D43**, 261 (1991).

[32] J.C. Collins, Nucl. Phys. **B396**, 161 (1993).

[33] (HERMES Collaboration) A. Airapetian *et al.*, Phys. Rev. Lett. **84**, 4047 (2000); Phys. Rev. **D64**, 097101 (2001).

[34] (HERMES Collaboration) A. Airapetian *et al.*, Phys. Rev. Lett. **94**, 012002 (2005).

[35] U. D'Alesio and F. Murgia, Prog. Part. Nucl. Phys. **61**, 394 (2008).

[36] D. L. Adams *et al.*, Phys. Lett. **B261**, 201 (1991).

[37] D. L. Adams *et al.*, Phys. Lett. **B264**, 462 (1991).

[38] J. Adams *et al.*, Phys. Rev. Lett. **92**, 171801 (2004).

[39] I. Arsene *et al.*, Phys. Rev. Lett. **101**, 042001 (2008).

[40] J. C. Collins and D. E. Soper, Phys. Rev. **D16**, 2219 (1977).

[41] S. Arnold, A. Metz, and M. Schlegel, Phys. Rev. **D79**, 034005 (2009).

[42] P. Hägler, B. Musch, J. Negele, and A. Schäfer, Europhys. Lett. **88**, 61001 (2009).

[43] B. U. Musch, P. Hägler, J. W. Negele, and A. Schäfer, Phys. Rev. **D83** 094507 (2011).

[44] P. Schweitzer, T. Teckentrup, and A. Metz, Phys. Rev. **D81**, 094019 (2010).

[45] (Spin@Fermi Collaboration) E.D. Courant, *et al.*, arXiv:1110.3042 [physics.acc-ph], "Updated Report Acceleration of Polarized Protons to 120-150 GeV/c at Fermilab", submitted to Fermilab in August 2011.

[46] M. Anselmino *et al.*, Phys. Rev. **D79**, 054010 (2009); plus private communications.

[47] (HERMES Collaboration) A. Airapetian *et al.*, Phys. Rev. Lett. **103**, 152002 (2009).

[48] (HERMES Collaboration) A. Airapetian *et al.*, Phys. Lett. **B693**, 11 (2010).

[49] (COMPASS Collaboration) M. Alekseev, *et al.*, Phys. Lett. **B673**, 127 (2009).

[50] A. Bacchetta and M. Radici, arXiv:1107.5755 [hep-ph].

[51] (COMPASS-II collaboration), http://wwwcompass.cern.ch/compass/proposal/compass-II_proposal/compass-II_proposal.pdf.

[52] (PAX Collaboration), V. Barone et al., arXiv:hep-ex/0505054.

[53] (PANDA Collaboration), http://www-panda.gsi.de/auto/_home.htm.

[54] (NICA Collaboration), http://nica.jinr.ru/.

[55] (RHIC Spin Collaboration), http://spin.riken.bnl.gov/rsc/write-up/dy_final.pdf.

[56] Y. Goto et al., http://indico.cern.ch/conferenceDisplay.py?confId=85721.

[57] (SeaQuest Collaboration) D. Geesaman, P. Reimer *et al.*, Fermilab Proposal P906 (1999); http://www.phy.anl.gov/mep/drell-yan.

[58] A. Zelenskiet al., "The RHIC Polarized H^- Source", *AIP Conference Proceedings* No. 1149, eds. D. Crabb, D. Day, S. Liuti, X. Zheng, M. Poelker, and Y. Prok, p. 847 (2009).

[59] A.S. Belov et al., private communications.

[60] J. C. Webb, *Measurement of continuum dimuon production in 800-GeV/c proton nucleon collisions*, Ph.D. thesis, New Mexico State University, 2003.

[61] D. Mack, *Outlook for Determining Beam Charge in Fermilab E906 with an Unser Monitor*, unpublished note, Projects-doc-442-v1, 5 Feb 2009.

[62] A. Zelenski *et al.*, Jour. Phys.: Conference Series **295**, 012132 (2001)

[63] A. Bazilevsky *et al.*, AIP Conf. Proc. **1149**, 723 (2009).